Ultra-narrow bandpass filters based on volume Bragg grating technologies

Julien Lumeau*[1], Vadim Smirnov[2], Alexei Glebov[2] and Leonid B. Glebov[1]

[1]School of Optics/CREOL, University of Central Florida, Orlando, FL 32816-2700, USA
[2]OptiGrate Corporation, 3267 Progress Drive; Orlando, FL, 32826, USA

ABSTRACT

Free space optical communication between movable platforms, especially communication with non-cooperative targets, requires detecting low intensity signals in conditions of multiple sources of contaminating signals. In this paper, we review recent achievements in ultra-narrow bandpass filters based on volume Bragg gratings (VBGs) recorded in the bulk of photo-thermo-refractive glass. The new types of transmission filters show unique characteristics such as high throughput and bandwidths as narrow as a few picometers at any wavelength from 500 to 2700 nm. The first filter type is formed by the incoherent combination of a Fabry-Perot etalon and a VBG that enables tunable ultra-narrow band transmission with a single resonance. The filters demonstrate a bandwidth down to a few picometers at 1064 nm, a transmission exceeding 90%, an ultra-broad rejection band (several hundreds of nanometers), and an extinction ratio better than 30 dB. The second filter type is based on multiplexed frequency shifted VBGs that form a volumetric Moiré Bragg grating. The filter provides a single resonance with transmission higher than 90% in the middle of the reflection lobe of the VBG, a bandwidth down to a few picometers and high mechanical stability. Both types of ultra-narrow bandpass filters can be used for many applications requiring to transmit a single frequency and to reject other adjacent frequencies, e.g., in Lidars, or for selection of longitudinal modes in laser resonators. The new filters provide a significant advantage in terms of stability, tunability and achievable throughput for a given bandwidth.

Keywords: Volume Bragg grating, Fabry-Perot, narrow band filter

1. INTRODUCTION

Free space optical communication between movable platforms, especially communication with non-cooperative targets, requires detecting low intensity signals in conditions of multiple sources of contaminating signals. Detecting such signals requires using of narrowband filters in order to separate useful signals from perturbing one. The most common technology for performing such a task uses optical interference filters [1]. Such filters are obtained by optical coating technology, i.e. deposition of a sequence of low and high refractive index materials on top of a substrate. However, in order to achieve complex functions with high efficiencies, it is required to deposit several hundreds of layer resulting in very thick stacks which are very sensitive to errors of depositions [2]. Despite the development of new type of optical controls associated reverse engineering processes [3], the fabrication of such filters, while possible, remains challenging and even more when aperture requires being increased to several centimeters or larger. One alternative for producing narrowband filters is the use of holographic optical elements (HOE) such as volume Bragg gratings. Such filters can be produced by holographic recording inside a photosensitive medium. Most popular media include dichromated gelatins [4], photorefractive crystals [5] and photopolymers [6]. However, these materials do not allow achieving high efficiencies, nor elements with low level of wavefront distortions of the diffracted beam. Moreover, holographic optical elements are not robust (HOE in photorefractive crystals tend to fade [7]), and are only suitable for very low power applications. 15 years ago, a new material was introduced as potential photosensitive materials for the recording of HOEs: photo-thermo-refractive (PTR) glass [8]. PTR glass is a Na_2O-ZnO-Al_2O_3-SiO_2 glass doped with silver (Ag), cerium (Ce), and fluorine (F). The photo-thermal-refractive process is based on precipitation of dielectric microcrystals of NaF in the glass bulk. The process requires several steps. The first step is an exposure of the glass wafer to near UV radiation to photo-excite cerium ions. The Ce^{3+} ions convert to Ce^{4+} and the release electrons are trapped by silver ions

Photonics in the Transportation Industry: Auto to Aerospace III, edited by
Alex A. Kazemi, Bernard C. Kress, Eric Y. Chan, Proc. of SPIE Vol. 7675, 76750H

converting them to neutral silver atoms. This second stage corresponds to a latent image formation in conventional photosensitive materials and no significant coloration or refractive index variations occur in PTR glass at this stage. The latent image corresponds to a distribution of silver atoms in the glass bulk that matches the energy dosage distribution of exciting radiation. The third stage is diffusion of silver atoms, which leads to creation of tiny silver containing particles at temperatures exceeding 460ºC. These silver containing particles serve as nucleation centers for sodium fluoride crystal growth at temperatures between 500 and 550˚C. It was found that after this fourth stage, the refractive index in the exposed area decreases by about 10^{-3} relative to the index in the unexposed area.

The window of complete transparency of PTR glass is from 350 to 2700 nm. The absorption edge in the UV region is formed by bands of cerium contained in PTR glass. Absorption at wavelengths greater 2700 nm is produced by hydroxyl groups contained in silicate glass as technological contaminations. UV-exposure and subsequent thermal development causes additional absorption in the visible region due to silver containing particles, but this absorption band be easily optically bleached. Fluoride crystals are colorless and therefore do not cause additional absorption but they cause induced scattering. In conclusion, typical absorption in near-IR regions in HOE in PTR glass does not exceed 5×10^{-4} cm^{-1} while scatterings losses range from 5×10^{-3} cm^{-1} to 2×10^{-2} cm^{-1} (i.e. less than a few % scattering in HOE) depending on the efficiency of the recorded element.

From the conventional optical point of view, PTR glass is a crown-type optical glass having a refractive index at 587.5 nm of n_d=1.4959 and Abbe number ν_δ=59.2. Thermal variations of refractive index in PTR glass are very low ($dn/dT=5\times10^{-8}$ 1/K). This feature leads to a thermal shift of Bragg wavelength in PTR diffractive gratings of 7 pm/K. The melting temperature of NaF crystals is almost 1000°C. This is why PTR holograms are stable at elevated temperatures. These diffractive elements tolerate thermal cycling up to 400°C. This temperature is determined by the plasticity of the silicate glass matrix.

In this paper, we review the recent achievements in ultra-narrow bandpass filters based on volume Bragg gratings (VBGs) recorded in the bulk of photo-thermo-refractive glass. The new types of transmission filters show unique characteristics such as high throughput and bandwidths as narrow as a few picometers at any wavelength from 500 to 2700 nm. We first review the actual level of the technology of reflecting Bragg gratings (RBG) and BragGrate™ Notch filter and describe some of the applications of such filters. Then we present a new type of filters which is formed by the incoherent combination of a Fabry-Perot etalon and a RBG that enables tunable ultra-narrow band transmission with a single resonance. Finally, we present a third type of filter based on multiplexed frequency shifted RBGs that form a volumetric Moiré Bragg grating.

2. REFLECTING BRAGG GRATINGS AND BRAGGRATE™ NOTCH FILTER

High efficiency reflecting Bragg gratings (RBGs) can be holographically recorded inside PTR glass using beams from a He-Cd laser. They are obtained by writing inside the photosensitive medium a sinusoidal refractive index modulation. Typical spectral dependence of the diffraction efficiency on incident wavelength is shown in figure 1. RBG are very narrowband reflecting filters. Diffraction efficiency can exceed 99.7%, bandwidths range from 30 to several hundreds of nanometers while angular acceptance is between 1 and 100 mrad and aperture of 35×35 mm^2 or more with very low wavefront distortions (λ/2) are within today's technological capabilities. Finally the technology of High Efficiency Volume Diffractive Elements in Photo-Thermo-Refractive Glass is protected by two issued patents [9-10]. High efficiency RBGs can be deployed as ultra-narrow bandpass and notch filters. They can be used for a variety of spectroscopic applications, for example, advanced Raman spectroscopy. Bandpass filters are formed from RBGs with diffraction efficiencies of about 95% and linewidths of 2-5 cm^{-1} at FWHM (i.e. between 80 and 200 pm at

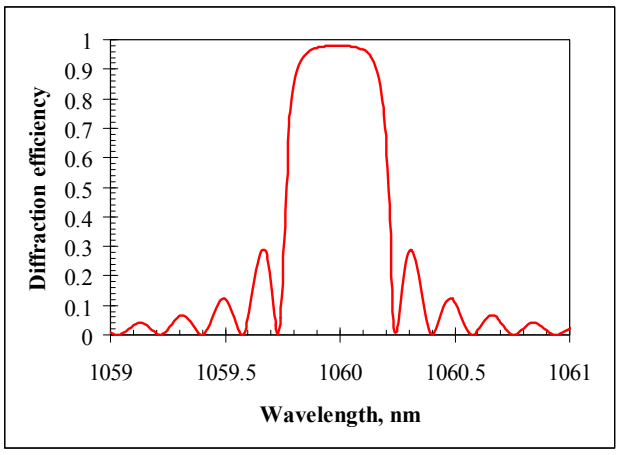

Figure 1. Typical spectral dependence of the diffraction efficiency on incident wavelength of a RBG.

633 nm). Since the filter is reflecting, it should be placed in a system accordingly, so that the reflected beam is directed to the sample under study and the "filtered out" signals are passed through and guided out of the critical areas. The available wavelength range of bandpass filters is 400-2500 nm, however, they are most frequently used for Raman applications: 1) ASE filtering of semiconductor laser diodes at 785 nm; 2) Cleaning of plasma lines of red HeNe lasers at 632.8 nm. Figure 2 demonstrates the performance of a 785 nm ASE filter. The "original" spectrum is from a multimode laser diode with spectral contrast of ~40 dB. After ASE filtering with an RBG bandpass filter, the spectral contrast is improved by more than 30 dB at 1 nm from the center of the laser line. The filter can be easily angle-tuned to the resonant wavelength in a several nanometers range without any performance degradation. It should be pointed out the line width of the cleaned laser is almost unaltered as compared to the original LD linewidth as the bandpass RBG band is as narrow as the one of the laser. Thus, VBG based bandpass filters enable laser beam cleaning as close as 2-5 cm^{-1} (i.e. between 120 and 300 pm at 785 nm) to the laserline center. Losses of such bandpass filters are mostly determined by the diffraction efficiency of the gratings and, therefore, are about 5%.

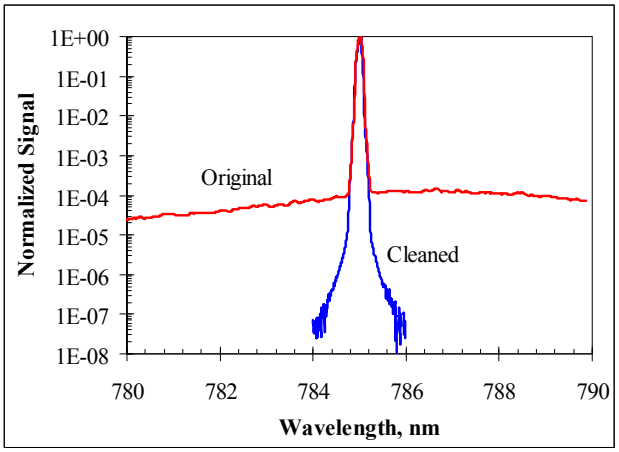

Figure 2. Performance of a narrow 785 nm bandpass filter from a standard RBG with 95% diffraction efficiency and bandwidth of about 3 cm^{-1}. The original spectrum is from a multimode 785 nm laser with the linewidth of about 150 pm.

High diffraction efficiency RBGs can also be used as BragGrate™ Notch Filters (BNFs) for Rayleigh light rejection in Raman spectroscopy. In this case, RBG efficiencies are maximized for most effective Rayleigh light suppression. Specially developed technology of high efficiency VBGs allows fabrication of 3-4 mm thick notch filters with optical densities OD>5 and line widths of 5-10 cm^{-1} at FWHM (i.e. between 300 and 600 pm at 785 nm). Typical commercially available single BNFs have OD3-4 and transmission of about 80-85% at 633 nm wavelength, and OD4-5 with transmission of about 90-95% at 785 nm. The filters are typically coated with broadband anti-reflective coating enabling low Fresnel reflectivities in the range from 400-1100 nm, therefore, providing good optical performance at Raman frequencies up to 5000 cm^{-1}.

Figure 3 shows suppression of 785 nm light from a multimode LD Raman light source. The laser beam is collimated with about 1 mm diameter and goes sequentially through a set of 2 notch filters. The first BNF rejects about 55 dB of the original light, while the second filter removes completely the residual signal around 785 nm. It is clearly seen that the line width of both BNFs is as narrow as that of the original laser.

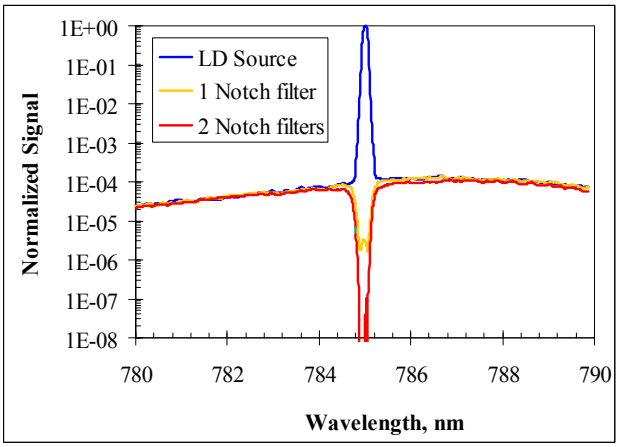

Figure 3. Suppression of 785 nm laser line with a set of 2 BragGrate™ Notch Filters (BNFs). Each filter has optical density higher than OD and the linewidth less than 10 cm^{-1}.

Such narrow band notch filters enable unique applications in ultra low wavenumber Raman spectroscopy. Typically, Stokes and anti-Stokes Raman excitation of 5-10 cm^{-1} are accessible only with triple monochromator stage systems, which are very bulky, expensive, and have rather low optical throughput. Recently we demonstrated with our partners that symmetrical Stokes and anti-Stokes Raman bands with frequencies less than 10 cm^{-1} can be measured simultaneously with only one stage monochromator Raman systems, thus, dramatically reduce the equipment size and cost as well as significantly boost the system optical throughput.

3. FABRY-PEROT-BRAGG FILTER

Fabry-Perot-Bragg (FPB) filters [11-12] are the first evolution of RBG/BNF that allows significant decrease of the bandwidth of the filter. FPBs are ultra-narrow bandpass filters. They consist of the incoherent combination of two optical components: a Fabry-Perot etalon (FPE) and a high-efficiency volume Bragg grating (VBG) recorded in photo-thermo-refractive (PTR) glass (figures 4-a and b). In these FPB filters, the FPE is used to define a comb of discrete narrow bands with desirable shape and bandwidth, while the volume Bragg grating which has a high spectral and angular selectivity is used to select only one of these bands. Due to the angular dependence of the central wavelength of a volume Bragg grating, it is possible to change its inclination and change the selected FPE resonance. Using this technique, the filter can be discretely tuned from one resonance to another. Properties of such filter are very robust, whatever the tuned wavelength due to the fact that maximum transmission, spectral width and rejection are mainly defined by the FPE and are constant over a broad range of wavelength. It is also possible to make FPB filters continuously tunable by tilting the FPE by a few degrees and shifting the central wavelength of the comb by one free spectral range. To achieve the desired spectral properties, several types of elements can be combined. Regarding the etalon, high finesse single cavity FPE can be used in order to achieve ultra-narrow bandpass and double cavity FPE can be used to achieve square profile and better rejection. Regarding the volume Bragg gratings they can be either a reflecting Bragg gratings (RBG) and in this case, the diffracted beam is on the same side than the incident beam, or a transmitting Bragg gratings (TBG) and in this case the diffracted beam is on the same side than the transmitted beam. To illustrate the typical properties of such filters, we present below two examples of such combination. The first case combines an ultra-narrowband single cavity FPE and a RBG while the second case combines a double cavity FPE and a RBG.

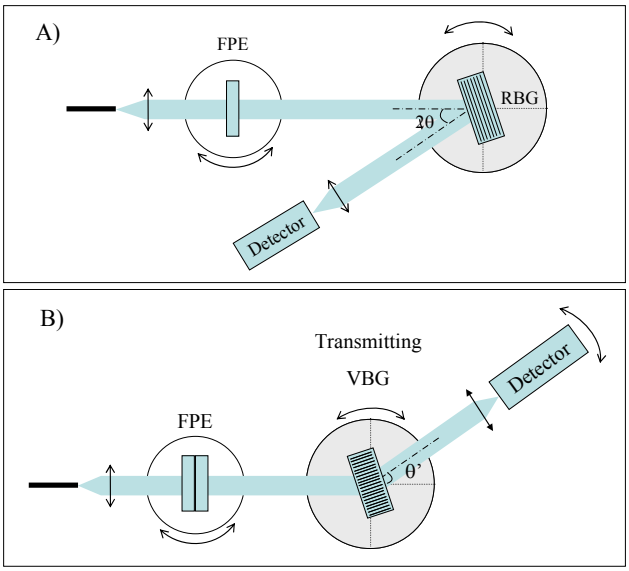

Figure 4. Fabry-Perot-Bragg filter geometry. A) is the case of the combination of a simple cavity FPE and a RBG. B) is the case of the combination of a double cavity FPE and a TBG.

1. Reflecting 25 pm bandwidth filter for 1060 nm region

A 25 pm bandwidth single cavity FPE with free-spectral range of 0.8 nm was combined with a RBG in order to obtain a reflecting ultra-narrowband Fabry-Perot-Bragg (FPB) filter. Throughput of the filter was measured for low inclination of the grating. In this case the filter is centered at 1064.9 nm. The spectral selectivity of the proposed narrow band filter resulting from the incoherent association of this RBG and the FPE is presented in Figure 5. Only one resonance appears in a wide spectrum. This unique narrow band resonance has a 25 pm bandwidth at FWHM. It can be seen that two small resonances ($T < 1\%$) are still visible close to the main resonance peak. To investigate in details the origin of these peaks, the inclination of the filter was changed in order to obtain a new coincidence between the FPE and the RBG at a different wavelength (~1055 nm). Then diffraction efficiency of the RBG and throughput of the FPB filter were recorded for the same RBG inclination. Measurements are represented in Figure 6. This graph

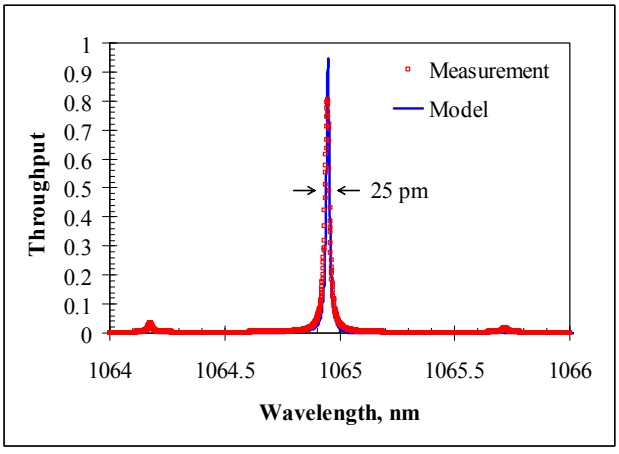

Figure 5. Throughput of the FPB filter for 1064 nm region, for low inclination of the RBG

demonstrates that rejection of the RBG is very efficient only about 6 nm away from the resonant wavelength. Outside this band, rejection is higher than 30 dB (detection limit of our measurement setup). Inside this 6-nm band, rejection is better than 30 dB except for 25 pm width narrow lines, equally separated by 0.8 nm and coinciding with the FPE resonances. At these resonant wavelengths, rejection is however better than 20 dB. Rejection close to the main peak can be severely improved by manufacturing a RBG with narrower line (such as 0.2 nm) and apodizing it. Moreover, according to the very low level of losses of the RBG, rejection can be severely improved by cascading two or more RBGs. Such solution would also have as consequence to avoid any rotation of the output beam when the RBG is rotated.

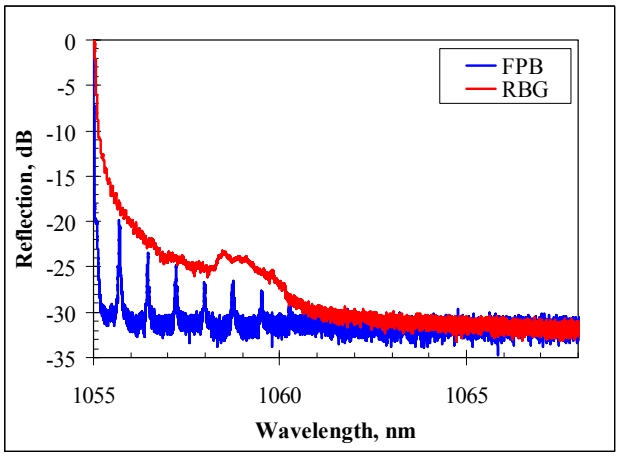

Figure 6. Throughput of the FPB filter for 1064 nm region, for larger inclination of the RBG. In blue, throughput of the FPB filter and in red the diffraction efficiency of the RBG.

As it was already introduced, the designed and manufactured FPB filters can be tuned by several tens of nanometers. RBG was originally centered at 1065.5 nm. However, the central wavelength of the RBG can be tuned to lower wavelengths by rotating it. Therefore, it is possible to select any resonant wavelength of the FPE by changing the inclination (rotating) of the RBG. Moreover, since the spectral response of the final filter is determined by the FPE, no distortion of this spectral response appears during tuning. Figure 7 shows the throughput of the filter measured for three different angles (~2.8°, ~7.9°, ~11.2°). Filter is shown to be tunable by 10+ nm without any spectral shape distortion and constant bandwidth equal to 25 pm. Moreover, even if only discrete tunability of our filter is shown here, continuous and fine tunability can be obtained if the inclination of the FPE is also adjusted to the desirable wavelength. According to the free spectral range of FPE which is limited to several tenths of nanometer, inclinations of the FPE of a few degrees would be enough to shift the whole comb by one free spectral range (FSR) and therefore tune to all the addressable wavelengths.

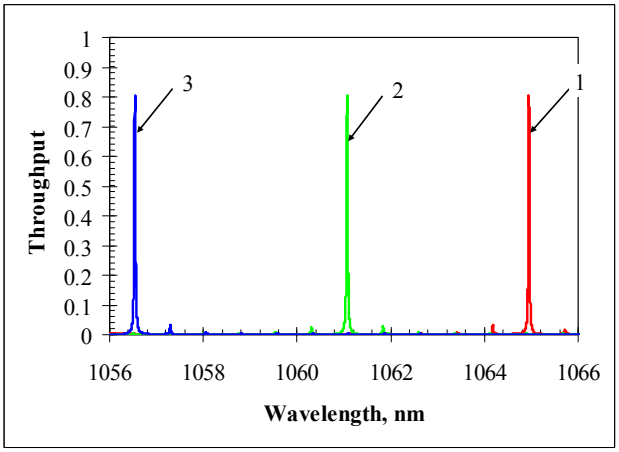

Figure 7. Throughput of the FPB filter for 1064 nm region, for different inclination (α) of the reflecting VBG: curve 1: α ~ 2.8°, curve 2: α ~ 7.9°, curve 3: α ~ 11.2°)

2. Transmitting double cavity filter for 1550 nm region

The second configuration of FPB filters consists in the combination of a double cavity FPE and a TBG. Throughput of the filter measured for one inclination of the TBG corresponding to a coincidence with a resonance of the FPE is shown in figure 8. TBG demonstrates a larger spectral selectivity than the RBG. Hence this justifies the use of FPE with large FSR in order to allow the TBG to select only one resonance of the FPE. The fabricated filter presents only one resonance which shape given by the FPE and throughput higher than 80%. Outside the resonance, the rejection is given by the product of the diffraction efficiency of the TBG and the transmission of the FPE. All remarks regarding improvement of the rejection (apodization, combining of two RBGs or TBGs) can be applied to this configuration too. Moreover, it is important to note that the fabricated FPB filter combines high spectral selectivity of a few tens or hundreds of picometers as defined by the FPE and high angular selectivity as defined by the TBG. FPB therefore capture the best of each element (FPE and VBG) and combines them into one unique filter. Finally, the filter can be tuned by several nanometers or tens of nanometers by changing the inclination of the TBG (figure 9).

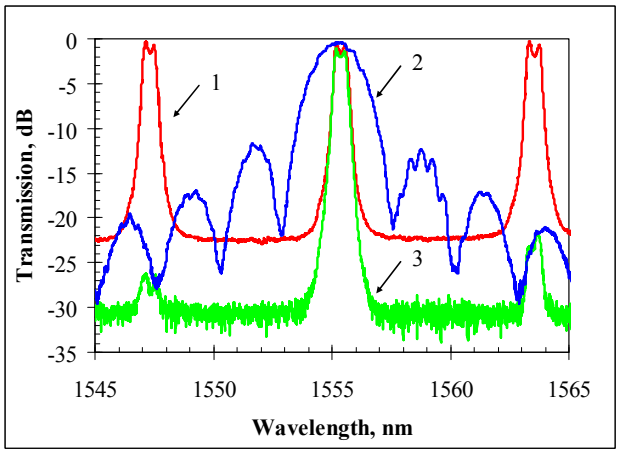

Figure 8. Throughput of the double cavity FPE (curve 1), the TBG (curve 2) and of the FPB filter (curve 3) for one inclination of the TBG.

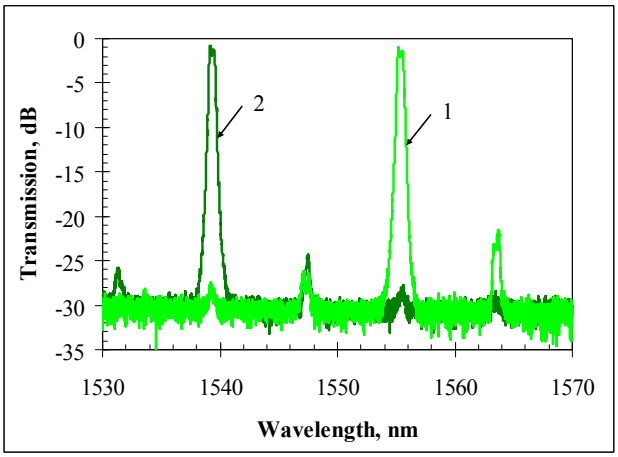

Figure 9. Throughput of the FPB filter for 1550 nm region, for 2 different inclinations of the TBG (curves 1 and 2).

4. MOIRE-BRAGG FILTER

FPB filters have shown to allow producing filters with very narrow bandwidth and broad range tunability. However, one of the main drawbacks of such configuration is that it is composed of two distinct elements and the fabrication of ultra-narrowband Fabry-Perot etalons is very expensive. Another alternative solution was recently proposed. It consisted in replacing both mirrors of the Fabry-Perot etalon with reflecting Bragg gratings and forming the equivalent of a π-shifted volume Bragg gratings [13]. Filter with bandwidth of 25 pm at 1064 nm was demonstrated. However, this combining was performed in air and therefore did not allow robust applications as required for laser systems. Last year, it was thus proposed to modify the structure of the filter and replace the physical π phase shift with a cancelation of the refractive index modulation in the middle of the filter, as obtained when generating a moiré pattern. A moiré pattern is an interference pattern created by two grids having slightly different periods. The phenomenon of Moiré pattern is illustrated by a well-known formula of trigonometry:

$$\cos(\alpha)+\cos(\beta)=2\cos\left(\frac{\alpha+\beta}{2}\right)\cos\left(\frac{\alpha-\beta}{2}\right) \tag{1}$$

Formula (1) shows that a combination of two elementary periodic functions with different periods results in a complex pattern which has a high frequency component with a period that is average between elementary periods and low frequency envelope with a period determined by the difference between elementary periods. When each grid is produced by the interference of two beams, we obtain the superposition of two shifted Bragg gratings and the recording of so-called moiré Bragg gratings (MBG) (figure 10). It is worth mentioning that the zero of the refractive index modulation is equivalent of a π-phase shift of the refractive index modulation. Such structure was widely investigated in the past in fibers [14]. However, due to the unavailability of bulk photosensitive materials with high optical homogeneity, no experimental demonstration of MBGs was performed. PTR glass allows recording of high

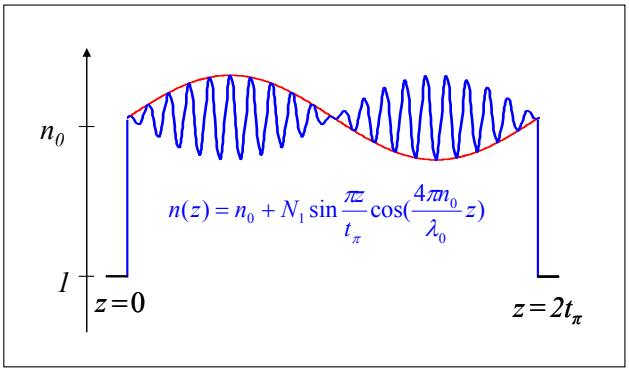

Figure 10. Spatial profile of refractive index modulation in a MBG with one Moiré period, i.e. two semi-periods with π phase shift between them.

efficiency reflecting Bragg gratings (RBGs) in a several millimeters thick glass sample and losses can be kept low below 1%. Hence, PTR glass makes an ideal candidate for the recording of a MBG with very high transmission at resonance [15]. For the recording, the beam from a single transverse mode He-Cd laser at 325 nm is expanded from 1 mm to 25 mm using 2 beam expanders. This beam is split into two beams with equal intensity. Both beams are reflected by two high quality mirrors and overlapped in the plane of recording (figure 11). Two gratings were recorded sequentially by changing of the incident angles of pairs of beams from 1-2 to 1'-2'. The period of each of the gratings (Λ_1, Λ_2) is determined by the angle between the two interfering beams inside of the photosensitive plate:

$$2n_0\Lambda_{1,2} = \frac{\lambda_R}{\sin(\theta_{1,2})} = \lambda_B \tag{2}$$

where n_0 is the refractive index of a recording medium, λ_R the wavelength of recording, θ the angle between the two beams inside the recording medium and λ_B the wavelength diffracted by the recorded grating at normal incidence along Z-axis in figure 11. It is therefore possible to change the period of the grating by changing the angle between the two beams. With high precision rotary stages, angle between the two beams can be controlled with precision better than 0.001°. The change of Bragg wavelength corresponding to such a change of angle is given by:

$$\Delta\lambda_B = \frac{\lambda_B}{\tan(\theta)}\Delta\theta \tag{3}$$

With such resolution, the shift of Bragg wavelength can be controlled with a precision better than 50 pm at 1 μm. As it will be shown later, such shift allows obtaining filter with bandwidth in the range of a few picometers in a few millimeters PTR glass substrates. By means of sequential two-beam recording with the same bisectors, the vector of a MBG can be perpendicular to the normal of the photosensitive plate surface, i.e. along the z axis in figure 11. A part of the recorded doubled grating with t_π thickness along Z-axis in figure 2 can be cut from the photosensitive plate to keep only one low-frequency period of the refractive index modulation for obtaining an ultra-narrowband transmitting filter.

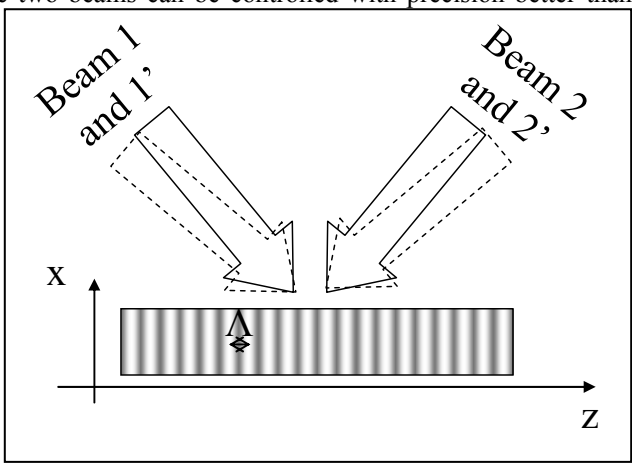

Figure 11. Sequential recording of a Moiré grating by two pairs of beams: 1-2 and 1'-2'.

To confirm these theoretical modeling, a MBG was experimentally demonstrated. The Moiré grating was recorded in a PTR glass wafer using the two-beam sequential technique described above. The two recorded RBGs had central wavelengths of 1547.2 and 1547.4 nm. The sample was thermally developed and then positions of zeros at the refractive index modulation profile were determined by scanning of a He-Ne laser beam with diameter of 1 mm along Z axis in figure 11. This sample was cut in the vicinity of the zeros of the refractive index modulation profile to thickness equal to 6 mm i.e. one low frequency period ($2t_\pi$) and then ground, polished and AR coated. Overall refractive index modulation was estimated in the range of ~120 ppm. Spectral selectivity of this Moiré grating was characterized. Typical spectral transmission measured at the throughput of the filter is shown in figure 12. This filter shows transmission higher than 95%. Bandwidth is equal to ~50 pm at FWHM and rejection

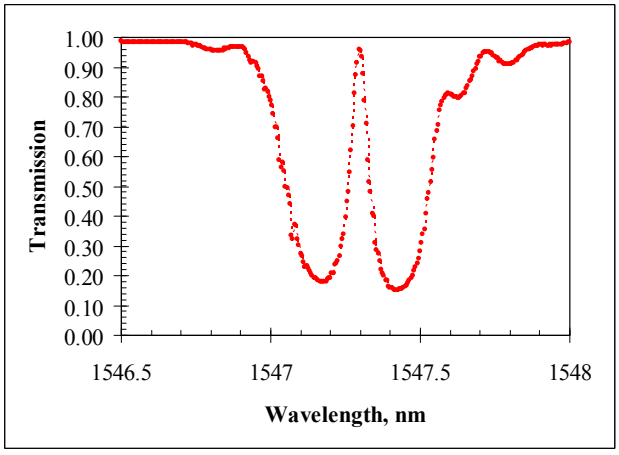

Figure 12. Experimental spectral selectivity of a Moiré grating recorded in PTR glass. Separation between resonant wavelengths of elementary RBGs – 200 pm. Thickness – 6 mm. Refractive index modulation – 120 ppm.

bandwidth to 200 pm. Rejection outside the resonance is in the range of 10 dB. Parameters of such a filter can be improved by optimization of a fabrication process and combining it with an additional RBG or by using a VBG with higher diffraction efficiencies in Ref. [11].

Let us now analyze the parameters of the RBG required to obtain an ultra-narrow bandpass filter centered in 1 μm region and with bandwidth at FWHM of a few picometers. Three main parameters define the final bandwidth of such a Moiré Bragg filter:

- The difference between periods of the two VBGs, i.e. difference between central Bragg wavelengths
- The thickness of the MBG
- The amplitude of refractive index modulation of each VBG

The dependence of spectral width (FWHM) of a transmission peak on thickness of the Moiré VBG for different values of refractive index modulation at constant separation between Bragg wavelengths (100 pm) is shown in Figure 13. For all simulations, we supposed that π phase shift occurs in the center of the Moiré grating, resulting in a symmetric and resonant filter. It is seen that for reasonable parameters of gratings, it is possible to fabricate a filter with a few picometers bandwidth for 1 μm region in a PTR glass with thickness less than 10 mm. Moreover, due to monolithic nature of the filter no problem of alignment between the two VBGs should be encountered.

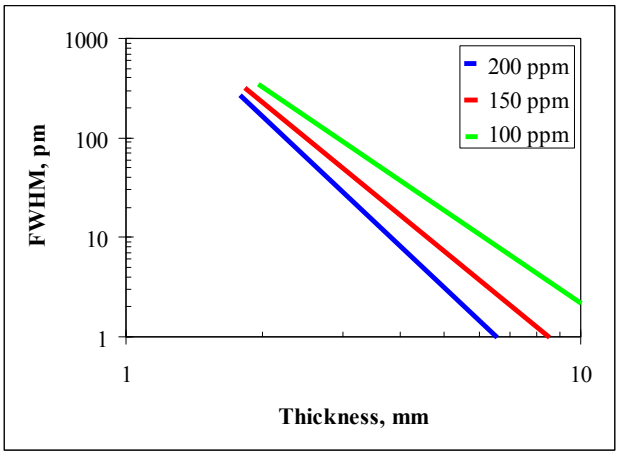

Fig. 13. Dependence of spectral selectivity (FWHM) of a Moiré grating on thickness for different values of refractive index modulation at constant separation between Bragg wavelengths of elementary RBGs of 100 pm.

5. CONCLUSION

In this paper, we have reviewed the recent achievements for decreasing the bandwidth of holographic optical elements recorded in photo-thermo-refractive glasses. We have first shown that reflecting Bragg gratings and BragGrate™ notch filters allow achieving high efficiency and bandwidth down to a few tens of picometers. Such filters find many applications in Lidars and laser systems. We demonstrated that two different approaches can be implemented in order to further decrease this bandwidth. The first one (Fabry-Perot-Bragg filters, FPB) consists in adding on the volume Bragg grating (VBG) beam path a Fabry-Perot etalon (FPE) that will allow producing a comb of ultra-narrow lines. In FPB filters, the VBG is then used only as selector for one of this line. Tunable filter with linewidth of a few picometers and with stable shape and throughput can be achieved using this technology. Tunability is based on the angular dependence of the FPE and the VBG on incident angle and is therefore performed by tilting of the VBG and/or the FPE to the desired wavelength. The second approach consists in combining the FPE and the VBG within one single element. Moiré-type structure was demonstrated in PTR glass. Using such element, filters with a few picometers bandwidth can be achieved at any wavelength from 400 to 2700 nm. The main advantage of such structure is that it is aligned during the recording and therefore cannot be misaligned after fabrication. Moreover, due to the ultra-low absorption level of PTR glass and its robustness to ionizing radiation, it makes an ideal candidate for selecting narrow lines in high power laser systems or in harsh conditions.

5. ACKNOWLEDGEMENTS

This work has been supported by NASA contracts NNL06AA42P and NNG07CA04C

6. REFERENCES

[1] H.A. Macleod, "Thin-Film Optical Filter" (Macmillan), third ed., Institute of Physics Pub., New York (2001).
[2] Dr. Turan Erdogan and Dr. Atul Pradhan, "Optical Filters Go Deeper", Photonics Spectra, (March 2008).
[3] Detlev Ristau, Henrik Ehlers, Tobias Gross, and Marc Lappschies, "Optical broadband monitoring of conventional and ion processes," Appl. Opt. 45, 1495-1501 (2006).
[4] B. J. Chang and C. D. Leonard, "Dichromated gelatin for the fabrication of holographic optical elements", Appl. Opt. 18, 2407–2417 (1979).
[5] James, S.W.; Dockney, M.L.; Tatam, R.P., "Photorefractive volume holographic demodulation of in-fiber Bragg grating sensors", Photonics Technology Letters, IEEE 8 (5), 664 – 666 (1996).
[6] Juan Manuel Russo and Raymond K. Kostuk, "PQ/PMMA holographic filters for OCDMA over CWDM applications", Proc. SPIE 7049, 70490R (2008).
[7] Cuixia Dai, Liren Liu, De_an Liu, Zhifang Chai, Zhu Luan, "Optimizations for the uniformity of the non-volatile volume grating in doubly doped LiNbO3 crystals", Optics Communications 248, 27–33 (2005).
[8] L.B. Glebov, "Photosensitive glass for phase hologram recording", Glastech. Ber. Glass Sci. Technol. 71C, 85-90 (1998).
[9] Oleg M. Efimov, Leonid B. Glebov, Vadim I. Smirnov, "High efficiency volume diffractive elements in photo-thermo-refractive glass", Patent No. US 6,673,497 B2. January 6, 2004.
[10] Oleg M. Efimov, Leonid B. Glebov, Larissa N. Glebova, Vadim I. Smirnov, "Process for production of high efficiency volume diffractive elements in photo-thermo-refractive glass" United States Patent 6,586,141 B1. July 1, 2003.
[11] J. Lumeau, V. Smirnov and L.B. Glebov, "Tunable narrow-band filter based on a combination of Fabry-Perot etalon and Volume Bragg Grating" *Optics Letters* **31** (16), 2417 – 2419 (2006).
[12] J. Lumeau, V. Smirnov, F. Lemarchand, M. Lequime and L.B. Glebov, "Large aperture tunable ultra narrow band Fabry-Perot-Bragg filter", *Proceeding of SPIE* **6469**, paper 64690M (2007).
[13] J. Lumeau, V. Smirnov, and L.B. Glebov, "Phase-shifted volume Bragg gratings in photo-thermo-refractive glass", *Proceeding of SPIE* **6890**, paper 68900A, (2008).
[14] R. Kashyap, "Fiber Bragg Gratings", *Academic Press*, 1st edition (May 15, 1999).
[15] V. Smirnov, J. Lumeau, S. Mokhov, B. Ya. Zeldovich and L.B. Glebov, "Ultra-narrow bandwidth Moiré reflecting Bragg gratings recorded in photo-thermo-refractive glass", *Optics Letters* 35 (4), 592–594 (2010).